Multistep Tandem Mass Spectrometry for Sequencing Cyclic Peptides in an Ion-Trap Mass Spectrometer

Lambert C. M. Ngoka and Michael L. Gross
Department of Chemistry, Washington University, St. Louis, Missouri, USA

Collisionally activated decomposition (CAD) of a protonated cyclic peptide produces a superposition spectrum consisting of fragments produced following random ring opening of the cyclic peptide to give a set of acylium ions (or isomeric equivalents) of the same *m/z*. Assignment of the correct sequence is often difficult owing to lack of selectivity in the ring opening. A method is presented that utilizes multiple stages of CAD experiments in an electrospray ion-trap mass spectrometer to sequence cyclic peptides. A primary acylium ion is selected from the primary product-ion spectrum and subjected to several stages of CAD. Amino-acid residues are sequentially removed, one at each stage of the CAD, from the C-terminus, until a b_2 ion is reached. Results are presented for seven cyclic peptides, ranging in sizes from four to eight amino-acid residues. This method of sequencing cyclic peptides eliminates ambiguities encountered with other MS/MS approaches. The power of the strategy lies in the capability to execute several stages of CAD upon a precursor ion and its decomposition products, allowing the cyclic peptide to be sequenced in an unambiguous, stepwise manner. (J Am Soc Mass Spectrom 1999, 10, 732–746) © 1999 American Society for Mass Spectrometry

Cyclic peptides comprise a large body of natural products and synthetic compounds. These peptides exhibit remarkable diversity and include antibiotics [1], toxins [2], immunosuppressants [3], ion-transport regulators [4], inhibitors of protein binding [5], and enzyme inhibitors [6]. They often possess unusual pharmacological properties of importance to biotechnology and medicine.

The determination of the structures of cyclic peptides by mass spectrometry has witnessed an evolution in concert with the developments in mass-spectrometry instrumentation and techniques. In 1982, an unknown peptide, a cyclic peptide, was sequenced by tandem mass spectrometry for the first time by Gross and co-workers [7]. In 1984, the same group [8] utilized high-energy, collisionally activated decomposition (CAD) in an effort to develop a general method to sequence cyclic peptides. It was then recognized that the determination of the amino-acid sequences of cyclic peptides by one stage of tandem mass spectrometry (MS/MS) was compromised by multiple and indiscriminate ring-opening pathways, resulting in a set of acylium ions of the same *m/z*. These acylium ions (or their isomeric equivalents) fragment, giving rise to product-ion spectra that are superpositions of spectra from fragmentation of the various ring-opened forms [8]. This is illustrated in Scheme **1** for a hypothetical cyclic peptide consisting of six amino-acid residues A, B, C, D, E, and F.

If all ring-opened isomers are formed, the product-ion spectrum would be a superposition of sets of the product ions shown at the right of the scheme. It would be relatively straightforward to assign the amino-acid sequences, realizing that all six primary acylium ions are actually present in the spectrum. In practice, however, not all amide bonds are broken, and there can be significant differences in the fragment-ion abundances. These differences may reflect the basicities of the amide nitrogens because an amide bond with a higher proton affinity may be more readily opened. This is the case with some proline-containing cyclic peptides when collisionally activated under high energy conditions; they afford selectivity by undergoing selective ring cleavage at the proline residue [8].

Eckart et al. [9] generalized the tandem-mass-spectrometry approach by separating the sequencing procedure into two different steps. The first step determines the connectivity between the amino-acid residues but does not give their orientations. The second step determines the orientation of the amino acids. The method, however, has limitations because several cyclic peptides with multiple dipeptide connectivities produced over-

Address reprint requests to Dr. M. L. Gross, Department of Chemistry, Washington University in St. Louis, One Brookings Drive, Campus Box 1134, St. Louis, MO 63130. E-mail: mgross@wuchem.wustl.edu

1044-0305/99/$20.00
PII S1044-0305(99)00049-5

Received February 8, 1999
Revised April 29, 1999
Accepted May 3, 1999

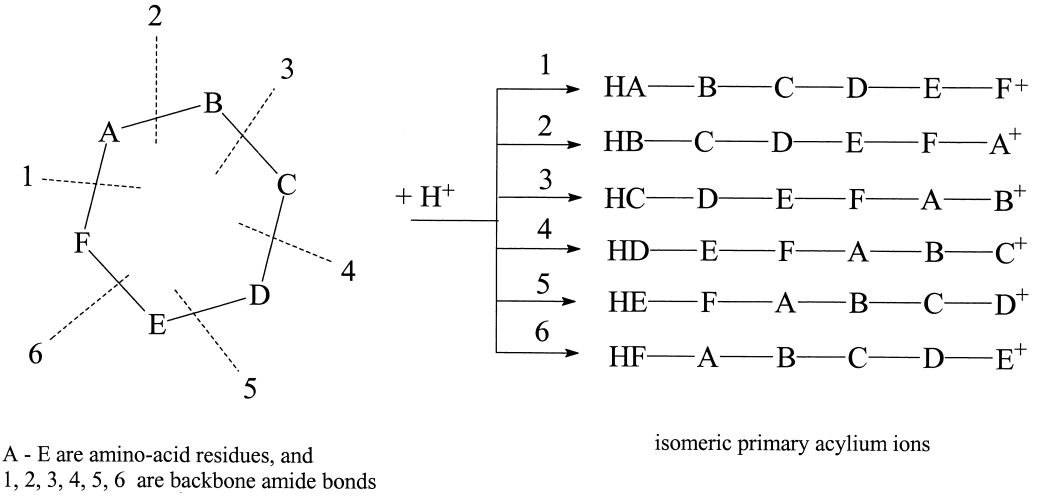

Scheme 1

lapping dipeptide and tripeptide fragments that are seen in the tandem mass spectra. These [10] and other related approaches [11, 12] have proven useful in sequencing several cyclic peptides.

The power of the nuclear-Overhauser-effect (NOE) techniques of NMR for assigning amino-acid sequences of cyclic peptides challenges mass spectrometrists to improve their approach. NOEs measured along the amide bonds of cyclic peptides furnish the structural detail, including correct assignments of the connectivity and orientation of the amino-acid residues [13–19]. Milligrams of highly purified material, however, are required for the NMR determination. Because cyclic peptides are usually produced by microorganisms, sufficient amounts of material may not be available. Therefore, there remains a strong need to improve the sensitive mass spectrometric methods.

In comparison with NMR, mass spectrometry has distinctive advantages of speed and sensitivity. Mass spectrometry is also suited to the analyses of mixtures. Because cyclic peptides lack free N-termini, they are not amenable to Edman degradation. Cyclic peptides generally contain large amounts of unusual and uncommon amino acids, which are synthesized by the microorganisms that produce them [10]. The challenge of structure determination has compelled many investigators to explore alternatives, some of which were mentioned above [8]. Another example is the work of Despeyroux et al. [20] who applied chemical reduction of cysteine-containing peptides in a reductive matrix prior to ionization by FAB. The amino-acid sequence of the resulting linear peptide was then determined by tandem mass spectrometry from the spectrum produced by the CAD of the $[M + H]^+$.

We report here a strategy incorporating multiple stages of collisionally activated decomposition in an electrospray-ionization (ESI), ion-trap mass spectrometer to determine amino-acid sequences of cyclic peptides. Multiple stages of consecutive CAD in an ion trap offer an opportunity to overcome the limitations caused by overlapping series of fragments in the tandem mass spectra of protonated cyclic peptides. Multiple stages of CAD were previously utilized in the determination of linkage positions in oligosaccharides [21, 22], in the distinction of isomeric polycyclic aromatic hydrocarbons [23], and the structure of complicated surfactants [24].

Experimental

Materials

Cyclo(Gln–Trp–Phe–Gly–Leu–Met) was purchased from BACHEM Bioscience, Inc. (King of Prussia, PA), cyclo(*D*-Asp–Pro–*D*-Val–Leu–*D*-Trp), cyclo(*D*-Asp–Pro–*D*-Ile–Leu–*D*-Trp), cyclo(*D*-Glu–Ala–*D*-*allo*Ile–Leu–*D*-Trp), cyclo(*D*-ser–Pro–*D*-Val–Leu–*D*-Trp), cyclo[Leu–*D*-Phe–Gly–*N*MeAla], and cyclo[Tyr–Phe–Gln–Asn–Asu]–Pro–Arg–Gly–NH_2 were purchased from Sigma Chemical Co. (St. Louis, MO) and were used without further purification.

Multistage Low Energy CAD of ESI-produced $[M + H]^+$ Ions

Electrospray experiments were carried out with a Finnigan LCQ ion-trap mass spectrometer (San Jose, CA) equipped with an ESI source. The spray needle was at a potential of 4.41 kV, and a 4800 kPa coaxial flow of nitrogen was used to stabilize the spray. The counter electrode was a heated (199 °C) stainless-steel capillary held at a potential of 10 V. The tube-lens offset was 65 V, and the electron multiplier voltage was −803 V. Helium gas was introduced into the ion trap at a pressure of 1 mtorr (measured on a remote ion gauge) to improve the trapping efficiency of the sample ions introduced into the ion trap. The background helium gas also served as the collision gas during the collisional

activation (CA) event. A typical experimental protocol consisted of infusing a 200–500 fmol/μL solution of a cyclic peptide solution in 20/80 MeOH/H_2O/1% formic acid into the mass spectrometer via a 250-μL syringe at a flow rate of 2 μL/min.

For experiments involving multiple stages of CAD, success depended on determining an optimum combination of the number of scans, isolation width, and relative collision energy. Of these parameters, the number of scans and isolation width were most important. The strategy in multiple CAD experiments was to use larger isolation widths (2–5 *m/z*) for the first stages of CAD to admit sufficient ions into the trap, whereas a narrow isolation width (~1 *m/z*) was used at the final CAD stage. The percentage relative collision energy was always adjusted such that the relative abundance of the precursor in the product-ion spectrum was approximately 10%–30%; generally the range of collision energy was 0.75–1.4 eV (laboratory frame). Spectra were acquired in the mass-profile mode, and the number of scans ranged from 2 to approximately 40, depending on the relative abundance of the precursor, the number of stages of CAD, and the nature of the sample.

The peptides were sequenced according to the following procedure. In the first stage, a protonated cyclic peptide was subjected to CAD to produce the first-generation, product-ion mass spectrum. In the MS^3 step, a given $b_{(n-1)JZ}$ ion (*b* is an acylium ion or equivalent and *n* is the number of amino-acid residues in the peptide as is discussed in the Nomenclature section at the end of the Experimental) was selected from the product-ion spectrum and then subjected to another stage of CAD. The resulting second-generation, product-ion spectrum (MS^3) contained sequence ions from $b_{(n-2)JZ}$ to b_{2JZ}. Next, $b_{(n-2)JZ}$ was selected from the spectrum of the second-generation, product ions and subjected to another stage of CAD to furnish the third-generation, product-ion spectrum (MS^4), ranging from $b_{(n-3)JZ}$ to b_{2JZ}. This procedure was repeated until the precursor ion had been reduced to b_{2JZ}, or the capability for further stages of CAD was exhausted owing to the loss of precursor-ion signal.

Sample amounts ranged from 1 to 100 pmol, depending on the number of stages and the size of the peptide. These quantities do not, however, represent detection limits, and no efforts were made to determine detection limit, ability to quantify, and other analytical issues.

High Energy CAD of FAB-produced $[M + H]^+$ Ions

High-energy CAD spectra of cyclo(*D*-Asp–Pro–*D*-Val–Leu–*D*-Trp), cyclo(*D*-Asp–Pro–*D*-Ile–Leu–*D*-Trp), and cyclo(*D*-ser–Pro–*D*-Val–Leu–*D*-Trp) were acquired on a VG ZAB-T four-sector instrument (Manchester, UK) [25]. The matrix, 0.5 μL of 3-nitrobenzyl alcohol (Aldrich Chemical Co., Milwaukee, WI), was placed on a FAB probe tip, and 0.5 μL of a 2-nmol/μL peptide solution in water was placed on the matrix drop. The sample was bombarded with a 25-keV cesium beam. The resulting gas-phase $[M + H]^+$ was accelerated to 8 keV and selected by MS1, which had been set at 1500 static resolving power (full width at half maximum). The collision cell was floated at 4 kV (0.5 of the acceleration potential). Helium gas was introduced into the collision cell at a pressure sufficient to attenuate the precursor-ion beam intensity to 50%. The resulting product-ion spectrum was acquired by scanning MS2, which was set at 1000 dynamic resolving power. The calibration of MS2 was accomplished by using CsI cluster ions that were generated in an intermediate source (after MS1) as references. Data acquisition and analyses were carried out with a VG (Manchester, UK) data system equipped with a DEC Alpha 3000 workstation, OPUS V 3.1X software, and a VG SIOS I interface.

Nomenclature

The nomenclature system is an extension of the Roepstorff and Biemann systems [26] and was used to label fragment ions. An ion is labeled with a four-part descriptor with the general formula x_{nJZ}, where "x" is the designation for the ion (lower case "a", "b", "c"). Thus, a b ion is the traditional acylium ion or isomeric equivalent, which may lose a carbon monoxide to form an a ion, and *n* is the number of amino-acid residues in the ion. J and Z are the one-letter (upper-case) codes for the two amino-acid residues connecting the backbone amide or ester bond, J–Z, that was broken to form the decomposing linear ion. J is the N-terminal amino-acid residue, and Z is the C-terminal amino-acid residue. The system requires ions to be uniquely identified as acylium ions, carbocations, cationized species, N-terminal and C-terminal ions, but does not specify the exact structures or origins of the ions.

Results and Discussion

Representative Cyclic Peptides

We present the CAD mass spectra of five representative cyclic peptides to illustrate the general approach in using multistep tandem mass spectrometry to sequence these materials.

Cyclo(Phe–Gly–Leu–Met–Gln–Trp). The product-ion spectrum of ESI-produced $[M + H]^+$ of cyclo(Phe–Gly–Leu–Met–Gln–Trp) (Figure 1) is illustrative of the difficulties in interpreting product-ion spectra of protonated cyclic peptides. We surmise that only two primary acylium ions, HTrp–Phe–Gly–Leu–Met–Gln^+ and HPhe–Gly–Leu–Met–Gln–Trp^+ are formed because only series of product ions originating from these precursors are seen. Three of the four remaining linear sequences, HGly–Leu–Met–Gln–Trp–Phe^+, HLeu–Met–Gln–Trp–Phe–Gly^+, and HMet–Gln–Trp–Phe–Gly–Leu^+, which can be formed by ring opening at other

cyclo(Trp—*Phe*—Gly—Leu—Met—Gln)

		b_{nWQ}		b_{nFW}		b_{nGF}		b_{nLG}		b_{nML}		b_{nQM}
6	Gln		Trp		Phe		Gly		Leu		Met	
5	Met	635	Gln	577	Trp	616	Phe	706	Gly	650	Leu	632
4	Leu	504	Met	449	Gln	430	Trp	559	Phe	593	Gly	519
3	Gly	391	Leu	318	Met	302	Gln	373	Trp	446	Phe	462
2	Phe	334	Gly	205	Leu	171	Met	245	Gln	260	Trp	315
1	Trp	187	Phe	148	Gly	58	Leu	114	Met	132	Gln	129

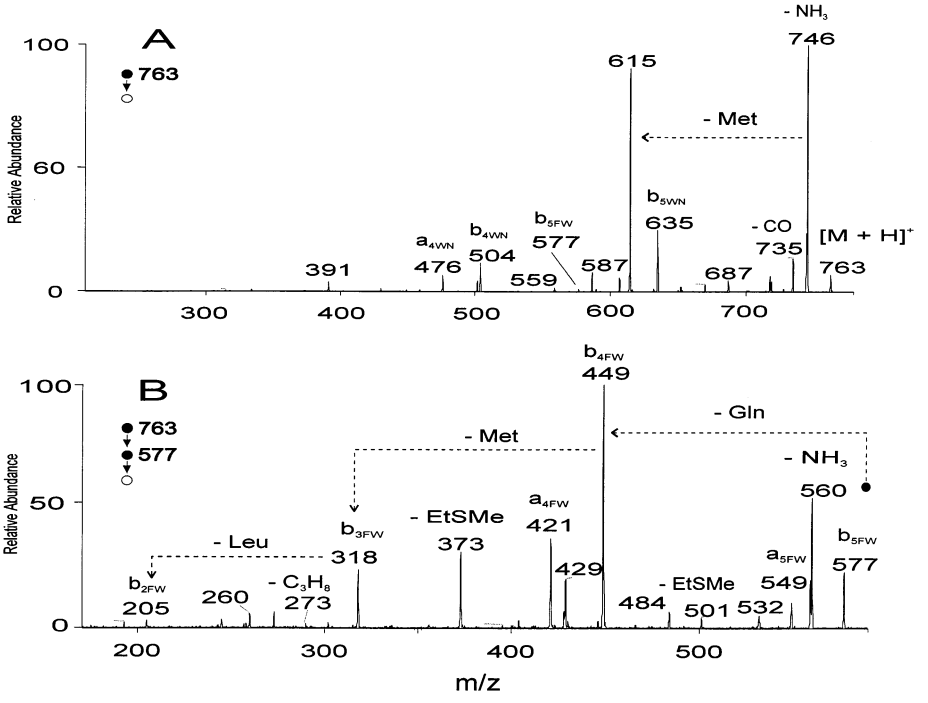

Figure 1. (**A**) First-generation, product-ion mass spectrum of protonated cyclo(Phe–Gly–Leu–Met–Gln). (**B**) Second-generation (MS^3) product-ion spectrum of the b_{5FW} ion HPhe–Gly–Leu–Met–Gln^+, formed by ring scission at the Phe–Trp amide bond.

amino-acid residues, are not detectable. There is evidence for the fourth sequence, HGln–Trp–Phe–Gly–Leu–Met^+, which may undergo loss of ammonia followed by sequential losses of Met (to give the *m/z* 615 ion) and Leu (to give the *m/z* 502 ion), underscoring the complexity endemic in first-generation, product-ion spectra of cyclic peptides.

The second-generation, product-ion spectrum of HPhe–Gly–Leu–Met–Gln^+, *m/z* 577 (Figure 1B) shows a set of sequence ions, down to b_{2FW}. This precursor ion was chosen to demonstrate the ability of the method to extract structural data from low-abundance ions. The amino-acid residues are preferentially lost from the C-terminus of the ring-opened acylium ion or equivalent, not from the N-terminus. Because we studied a limited number of cyclic peptides, we cannot yet conclude that this is a general phenomenon.

Endothelin A (ET_A) selective receptor antagonist cyclo(D-Asp–Pro–D-Val–Leu–D-Trp). The set of spectra for sequencing endothelin A (ET_A) selective receptor antagonist, cyclo(*D*-Asp–Pro–*D*-Val–Leu–*D*-Trp), cyclic peptide, is shown in Figure 2. Figure 2A is the first-generation, product-ion spectrum of the protonated molecule, showing a superposition of random fragments arising from five possible ring-opened, linear sequences. Figure 2B,C are the results of consecutive multistep CAD experiments, showing stepwise fragmentation of the acylium ion (or equivalent), HPro–Val–Leu–Trp^+, to furnish sequence to b_{2PD} at *m/z* 197. These experiments indicate that cyclo(*D*-Asp–Pro–*D*-Val–Leu–*D*-Trp) fragments nearly exclusively by stepwise scission of amino acid residues from the C-terminal side of the peptide, and that no detectable competing N-terminal fragmentation occurs.

The b_{2PD} ion is stable, and the fourth order (MS^5) CAD spectrum of the ion (not shown) does not produce the protonated proline residue (b_{1PD}); instead, an uninformative loss of carbon monoxide forms an a_{2PD} at *m/z* 169. Even MS^6, which was designed to look at the a_{2PD} ion of *m/z* 169, produced only the immonium ion of proline at *m/z* 70 instead of b_1: [a_{2PD} *m/z* 169, MS^6] →

[*m/z* 70 (100%)]. The inability to detect the b_{1PD} ion is consistent with the stability of b_2 ions [27]. This outcome does not allow the order of the first two amino acids (whether Pro–Val or Val–Pro) to be ascertained, leaving the connectivity of the amino acid residues as: Pro–Val–Leu–Trp–Asp or Val–Pro–Leu–Trp–Asp. One approach to resolve this ambiguity is to obtain the CAD mass spectrum of a reference a_2 ion *m/z* 169, generated from a standard reference Pro–Val dipeptide. Its product-ion mass spectrum is nearly identical to that of the a_2 ion generated from multistep CAD experiments (MS^6) on HPro–Val–Leu–Trp^+ (Figure 2A,B,C): [a_2 *m/z* 169, MS^3] → [*m/z* 70 (100%)]. As further confirmation, we obtained the CAD spectrum of a reference a_2 ion at *m/z* 169, generated from the reference Val–Pro dipeptide, and found that the spectrum was different from that of the a_2 ion from the reference Pro–Val dipeptide. We discuss later in this article another approach to this problem.

Endothelin A (ET_A) selective receptor antagonists cyclo(D-Asp–Pro–D-Ile–Leu–D-Trp) and cyclo(D-Ser–Pro–D-Val–Leu–D-Trp). It would be instructive to know how the fragmentation chemistry behind the foregoing spectra of cyclo(*D*-Asp–Pro–*D*-Val–Leu–*D*-Trp) would be affected if any amino-acid residue is replaced with a different one. If the method is general, the results should be predictable, regardless of the amino-acid composition of the cyclic peptide. Moreover, if our hypothesis is correct that low-energy collisional activation causes predominate fragmentation at the acylium-ion terminus, then it is important to initiate an experimental test that the observed fragmentation pathways are not related to the type of amino-acid residues at the N- and C-terminal ends of the decomposing ring-opened cyclic peptides. We repeated the high order MS/MS experiments by using two cyclic peptides in which the Val and Asp residues were substituted with Ile and Ser, respectively. When Val was replaced with Ile, the peptide has the structure cyclo(*D*-Asp–Pro–*D*-Ile–Leu–*D*-Trp), and the cyclic peptide is a powerful ET_A selective receptor antagonist. Its product-ion mass spectra are shown in Figure 3A,B,C, and for the cyclic peptide in which Asp is replaced with Ser, cyclo(*D*-Ser–Pro–*D*-Val–Leu–*D*-Trp), the product-ion spectra are shown in Figure 4A,B,C,D.

The product-ion mass spectrum of protonated cyclo(*D*-Asp–Pro–*D*-Ile–Leu–*D*-Trp) (Figure 3A) is a superposition spectrum consisting of fragments arising from random ring-opening pathways. One ring-opening pathway, the scission of the Asp–Pro amide bond to form HPro–Ile–Leu–Trp–Asp^+, was interrogated in consecutive, multistep CAD experiments. The third-generation, product-ion spectrum (Figure 3) shows the amino-acid sequence down to b_{2PD} at *m/z* 211. The spectrum is dominated, however, by the *m/z* 466 ion formed by loss of the elements of C_3H_8. In the MS^4 experiment, the b_{3PD} ion at *m/z* 324 was selected and collisionally activated to yield a highly abundant b_{2PD} ion at *m/z* 211 (Figure 3C). Collisional activation of the b_{2PD} ion in an MS^5 step produced only the a_{2PD} ion at *m/z* 183. In the MS^6 step, with a_{2PD} ion as the precursor, only the immonium ions of Pro and Ile were produced: *m/z* 70 (100%) and 86 (20%), respectively.

To determine the orientation of the N-terminal dipeptide (whether Pro-Ile or Ile-Pro), we obtained the CAD mass spectrum of a reference a_2 ion of *m/z* 183 from a reference Pro-Ile dipeptide. The spectrum is nearly identical to that of the a_{2PD} ion (of *m/z* 183) obtained from the multistep CAD (MS^6) experiments, starting with HPro–Ile–Leu–Trp^+ of Figure 3A,B,C. In contrast, the CAD spectrum of an ion with the retro sequence generated from the dipeptide Ile–Pro is different from that of Pro–Ile: a_2 (*m/z* 183, MS^4) → [*m/z* 155 (100%), *m/z* 138 (0.6%), *m/z* 127 (0.9%), *m/z* 115 (0.6%), *m/z* 88 (0.5%), *m/z* 86 (0.5%), *m/z* 70 (1%)].

A similar set of multistep CAD experiments (up to MS^6 ending with the a_{2PS} ion at *m/z* 169) was carried out on cyclo(*D*-Ser–Pro–*D*-Val–Leu–*D*-Trp) (Figure 4A,B,C), using the primary acylium ion or equivalent HPro–*D*-Val–Leu–*D*-Trp–*D*-Ser^+ (as will be established from the MS^n experiments). The type of fragmentation observed is identical to that of cyclo(*D*-Asp–Pro–*D*-Ile–Leu–*D*-Trp) of Figure 3. The experiments demonstrate that the fundamental fragmentation chemistry is the same for all three cyclic peptides: amino acid residues are sequentially removed from the C-terminus. In contrast to the high-energy CAD of proline-containing cyclic peptides [8], no preferential ring opening occurred at the proline residue.

These experiments on closely related peptides also enabled us to rationalize the identity and origin of the abundant ion at *m/z* 452 in Figure 2B. This ion is formed by the loss of the elements of C_3H_8 from the precursor ion of *m/z* 496. There are two possible sources of C_3H_8. One is loss of the entire valine side chain accompanied by H transfer to form an ion that is similar to a v ion [28–31] except it is missing the C-terminal OH. The product ion should be especially stable because it contains an α,β-unsaturated carbonyl moiety. The elements of C_3H_8 can also be eliminated from the side chain of Leu to form a d_{3PD} ion [28–31] but by a mechanism that is different than that pertaining to high-energy collisional activation. When Val was replaced with Ile (Ile cannot lose C_3H_8), the loss of C_3H_8 still occurs to give the ion of *m/z* 466 (Figure 3B). This is evidence that this loss is from the side chain of Leu and not that of Val.

High energy CAD of FAB-produced $[M + H]^+$ ions. We examined the high-energy CAD of the $[M + H]^+$ of proline-containing cyclic peptides cyclo(*D*-Asp–Pro–*D*-Val–Leu–*D*-Trp) (Figure 5A), cyclo(*D*-Asp–Pro–*D*-Ile–Leu–*D*-Trp) (Figure 5B), and cyclo(*D*-ser–Pro–*D*-Val–Leu–*D*-Trp) (Figure 5C). This was done to achieve a reference point demonstrating that the set of cyclic peptides chosen for our study does not have special properties but rather behaves in the expected way by

cyclo(*D*-Trp—*D*-Asp—Pro—*D*-Val—Leu)

		b_{nDW}		b_{nPD}		b_{nVP}		b_{nLV}		b_{nWL}
5	Trp		Asp		Pro		Val		Leu	
4	Leu	425	Trp	496	Asp	514	Pro	512	Val	498
3	Val	312	Leu	310	Trp	399	Asp	415	Pro	399
2	Pro	213	Val	197	Leu	213	Trp	300	Asp	302
1	Asp	116	Pro	98	Val	100	Leu	114	Trp	187

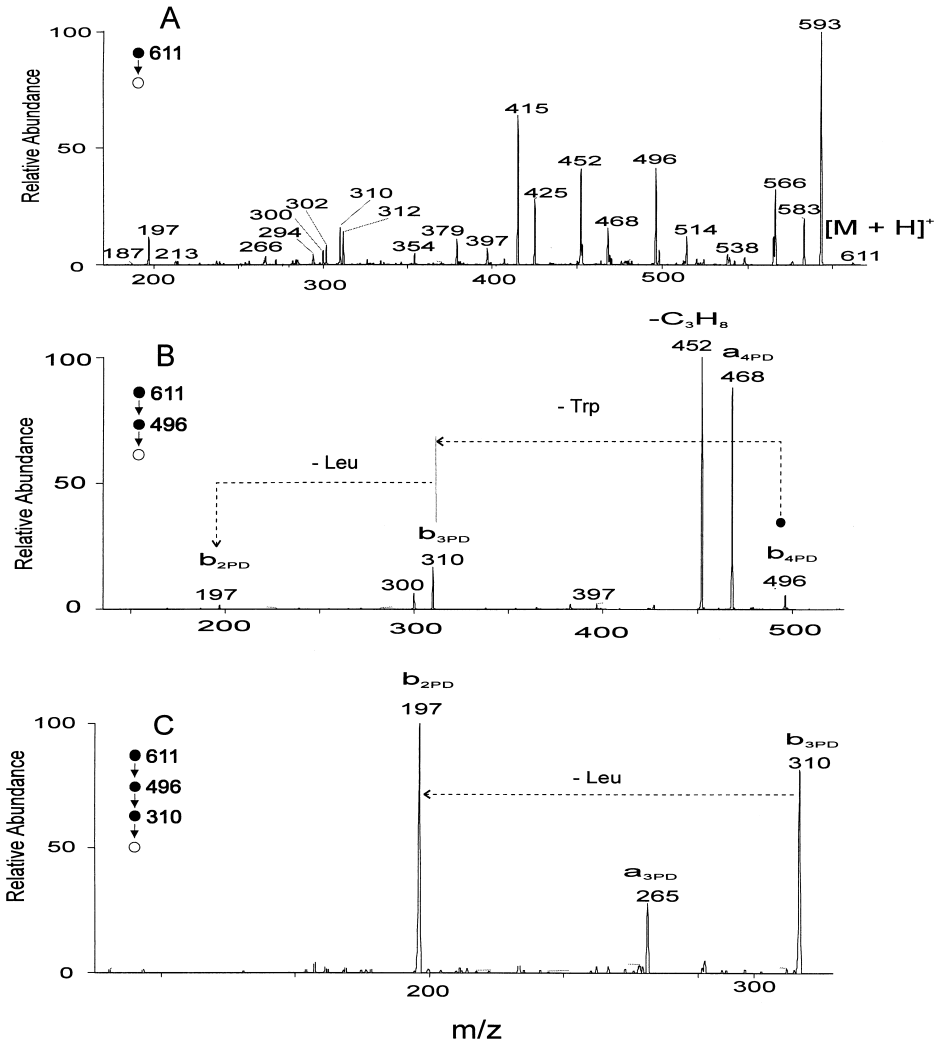

Figure 2. Multistep CAD mass spectra of cyclo(Asp–Pro–Val–Leu–Trp). (**A**) First-generation, product-ion mass spectrum of the protonated molecule. (**B**) Second-generation (MS^3), product-ion spectrum of the b_{4PD} ion HPro–Val–Leu–Trp$^+$ formed by ring scission at the Pro–Asp amide bond. (**C**) Third-generation (MS^4) product-ion spectrum of the b_{3PD} ion, HPro–Val–Leu$^+$

high-energy CAD. Indeed, high-energy collisional activation causes extensive fragmentation, underscoring the need for an alternative approach for sequencing cyclic peptides. The product-ion spectra show formation of highly abundant, low-mass fragments and low-abundance, high-mass ions. Indiscriminate ring opening, even for cyclic peptides containing proline [8], occurs. Ring opening at Pro is not dominant contrary to the high-energy collisional activation of proline-containing cyclic peptides that were previously studied [7, 8]. Thus, this set of cyclic peptides is an appropriate test of the capability of multistep, low-energy CAD.

Cyclic Peptides Containing Two or More Adjacent Amino-Acid Residues That Are Identical

Multiple stages of CAD are especially effective in resolving isobaric ions that occur in tandem mass spectra when the precursor ion contains several adjacent amino-acid residues that are identical or isomeric. For example, the ion at *m/z* 500 (loss of 113 Da from the protonated molecule) in the CAD mass spectrum of cyclo(*D*-Glu–Ala–*D*-*allo*Ile–Leu–*D*-Trp) (Figure 6) is likely to be a mixture of two isobaric ions formed by the loss of either Ile or Leu to give identical *m/z* product

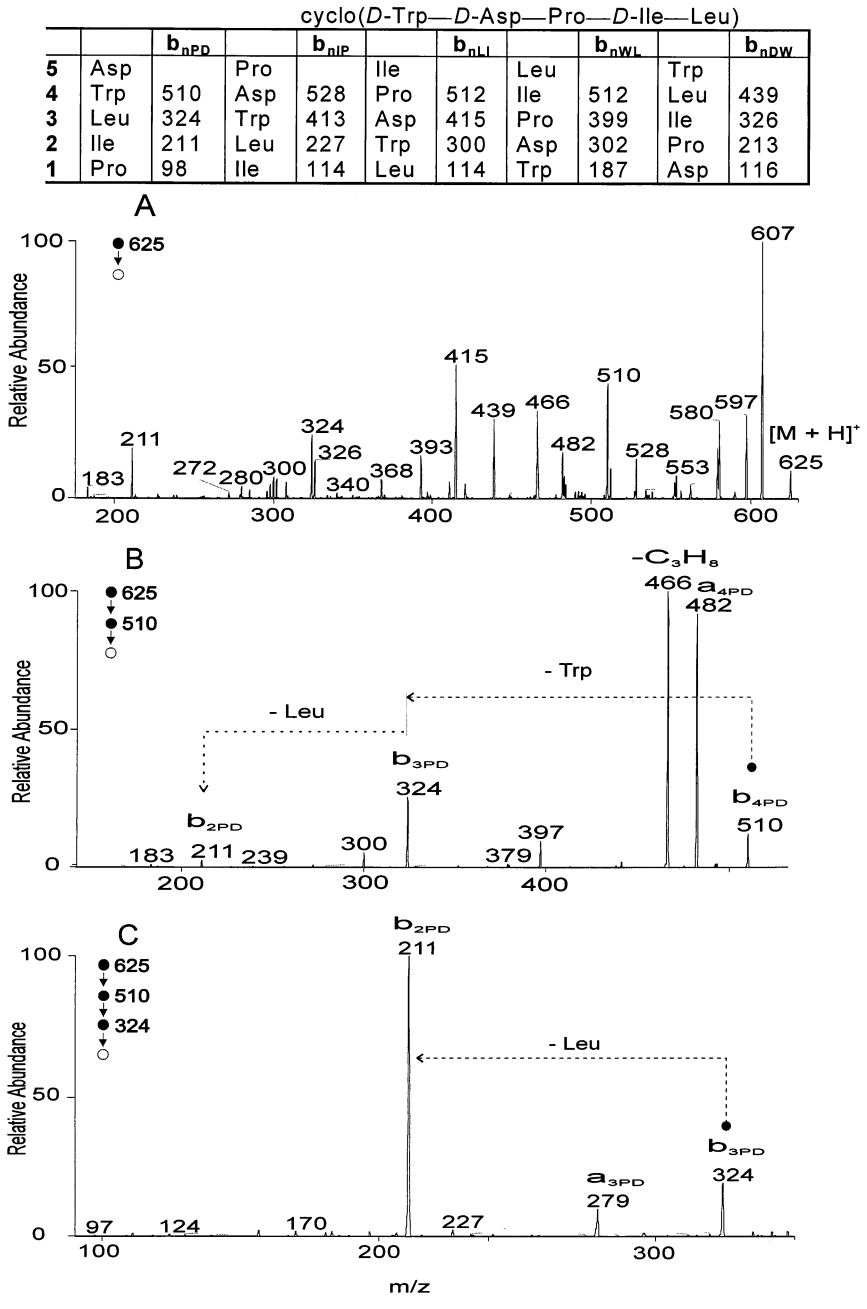

		b_{nPD}		b_{nIP}		b_{nLI}		b_{nWL}		b_{nDW}
5	Asp		Pro		Ile		Leu		Trp	
4	Trp	510	Asp	528	Pro	512	Ile	512	Leu	439
3	Leu	324	Trp	413	Asp	415	Pro	399	Ile	326
2	Ile	211	Leu	227	Trp	300	Asp	302	Pro	213
1	Pro	98	Ile	114	Leu	114	Trp	187	Asp	116

Figure 3. Multistep CAD spectra of cyclo(Asp–Pro–Ile–Leu–Trp). (**A**) First-generation, product-ion spectrum of the protonated molecule. (**B**) Second-generation (MS^3), product-ion spectrum of the b_{4PD} ion HPro–Ile–Leu–Trp^+ formed by ring scission at the Pro–Asp amide bond. (**C**) Third-generation (MS^4), product-ion spectrum of the b_{3PD} ion, HPro–Ile–Leu^+

ions. When the *m/z* 500 ion was selected as a precursor in an MS^3 experiment, two sets of amino-acid sequence ions, arising from the fragmentation of the linear acylium ions (or isomeric equivalents) HLeu–Trp–Glu–Ala^+ and HTrp–Glu–Ala–Ile^+, were obtained (Figure 6B). The two fragmentation pathways can be easily resolved in a consecutive stage of MS/MS, and the cyclic peptide can be sequenced without ambiguity.

Complete Connectivity of Amino-Acid Residues Can be Obtained by Sequencing Two Ring-Opened Forms of the Protonated Molecule

The CAD mass spectra of cyclo(*D*-Ser–Pro–*D*-Val–Leu–*D*-Trp) (Figure 4) show that the final stage of connectivity cannot be established by following one series of fragments because the b_{2PS} ion cannot fragment further

cyclo(*D*-Trp—*D*-Ser—Pro—*D*-Val—Leu)

		b_{nPS}		b_{nVP}		b_{nLV}		b_{nWL}		b_{nSW}
5	Ser		Pro		Val		Leu		Trp	
4	Trp	496	Ser	486	Pro	484	Val	470	Leu	397
3	Leu	310	Trp	399	Ser	387	Pro	371	Val	284
2	Val	197	Leu	213	Trp	300	Ser	274	Pro	185
1	Pro	98	Val	100	Leu	114	Trp	187	Ser	88

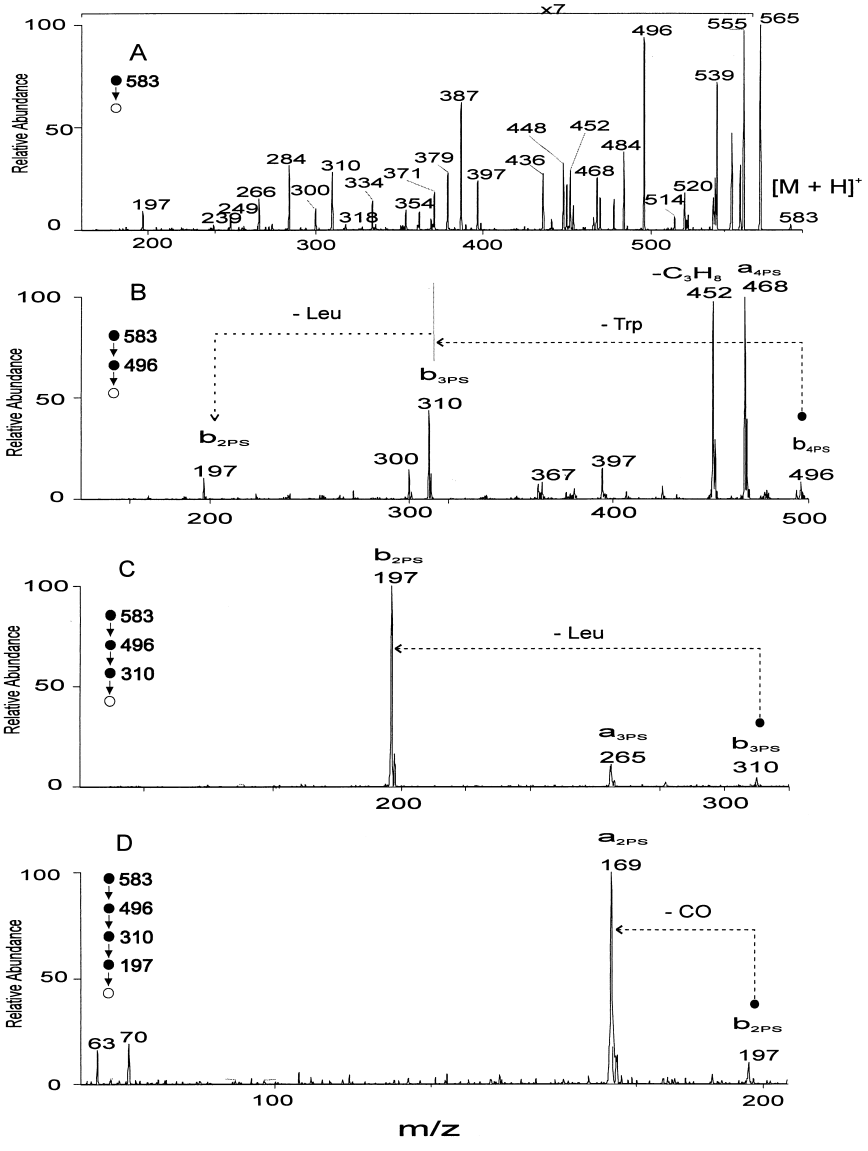

Figure 4. Multistep CAD mass spectra of cyclo(Ser–Pro–Val–Leu–Trp). (**A**) First-generation, product-ion mass spectrum of the protonated molecule. (**B**) Second-generation (MS^3), product-ion spectrum of the b_{4PS} ion HPro–Val–Leu–Trp^+ formed by ring scission at the Pro–Ser amide bond. (**C**) Third-generation (MS^4), product-ion spectrum of the b_{3PD} ion HPro–Val–Leu^+. (**D**) Fourth-generation (MS^5), product-ion spectrum of the b_{2PS} ion, HPro–Val^+.

to produce b_{1PS}. One approach to determining full connectivity is to obtain for comparison the CAD spectra of reference ions, as for the CAD spectra shown in Figures 2 and 3. Another approach for resolving the problem is to sequence at least two isomeric, ring-opened $[M + H]^+$ ions, as illustrated by a study of cyclo(*D*-Glu–Ala–*D*-*allo*-Ile–Leu–*D*-Trp) (Figure 6).

Figure 6A is the first-generation, product-ion spectrum, showing a superposition of fragment ions arising from indiscriminate ring-opening pathways. Figure 6B is the product-ion spectrum of both HTrp–Glu–Ala–Ile^+ (*m/z* 500) and HLeu–Trp–Glu–Ala^+ (*m/z* 500). By selecting the *m/z* 387 ion for additional MS/MS, we are able to sequence the former acylium ion and see sequential losses down to b_{2WL} ion at *m/z* 316. To sequence the latter ion, HLeu–Trp–Glu–Ala^+, we chose the *m/z* 429

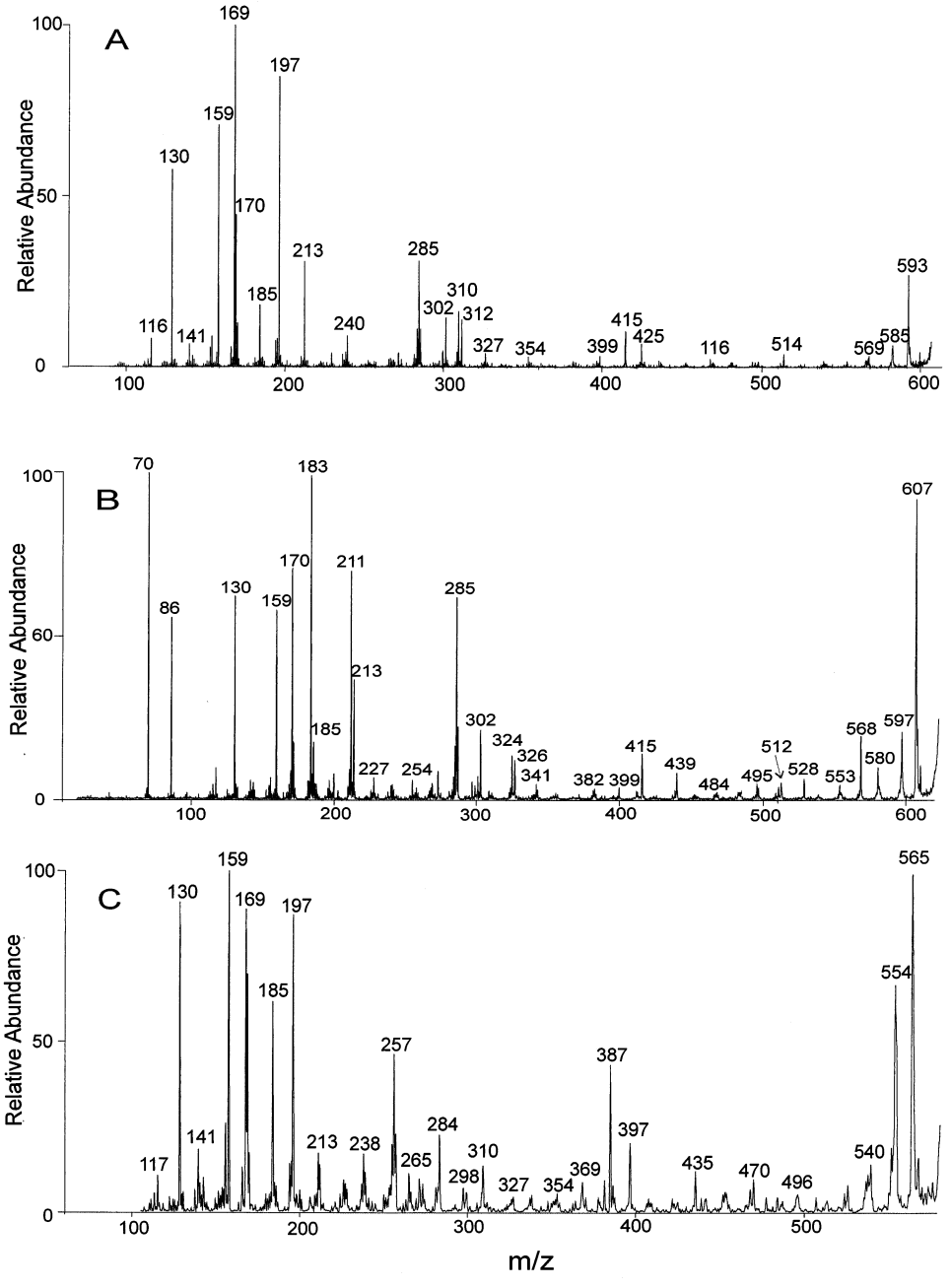

Figure 5. High-energy CAD spectra of the $[M + H]^+$ of proline-containing cyclic peptides cyclo(*D*-Asp–Pro–*D*-Val–Leu–*D*-Trp) (**A**), cyclo(*D*-Asp–Pro–*D*-Ile–Leu–*D*-Trp) (**B**), and cyclo(*D*-ser–Pro–*D*-Val–Leu–*D*-Trp) (**C**). The notable ammonium ions for Pro and Leu are missing in (**A**) and (**C**) because the scans were terminated at m/z values that are greater than *m/z* 86.

ion, and it manifests the expected fragmentation processes down to the b_{2LI} at *m/z* 300 (spectra not shown).

The question that remains is the sequence of the last two residues: is it Leu–Trp or Trp–Leu? The complete connectivity can be established by sequencing another ring-opened form; for example, the *m/z* 427 ion (formed by loss of Trp from HGlu–Ala–Ile–Leu–Trp^+), which can be selected from the first-generation, product-ion spectrum of Figure 6A. A major fragmentation of the *m/z* 427 ion is loss of Leu, establishing that the sequence is Leu–Trp. This connectivity could never be established with any confidence by interpreting the product-ion spectrum of the parent $[M + H]^+$, given the low relative abundances of the relevant ions in Figure 6A. The multistep spectra reveal the following processes: b_{4EW} (*m/z* 427, MS^3) → [*m/z* 409 (52%), *m/z* 399 (100%), *m/z* 381 (20%), *m/z* 342 (19%), b_{3EW}, *m/z* 314 (70%), *m/z* 292 (40%), *m/z* 268 (5%), *m/z* 243 (6%), *m/z* 227 (20%), b_{2EW}, *m/z* 201

cyclo(*D*-Trp—*D*-Glu—Ala—*D*-*allo*Ile—Leu)

		b_{nAE}		b_{nIA}		b_{nLI}		b_{nWL}		b_{nEW}
5	Glu		Ala		Ile		Leu		Trp	
4	Trp	484	Glu	542	Ala	500	Ile	500	Leu	427
3	Leu	298	Trp	413	Glu	429	Ala	387	Ile	314
2	Ile	185	Leu	227	Trp	300	Glu	316	Ala	201
1	Ala	72	Ile	114	Leu	114	Trp	187	Glu	130

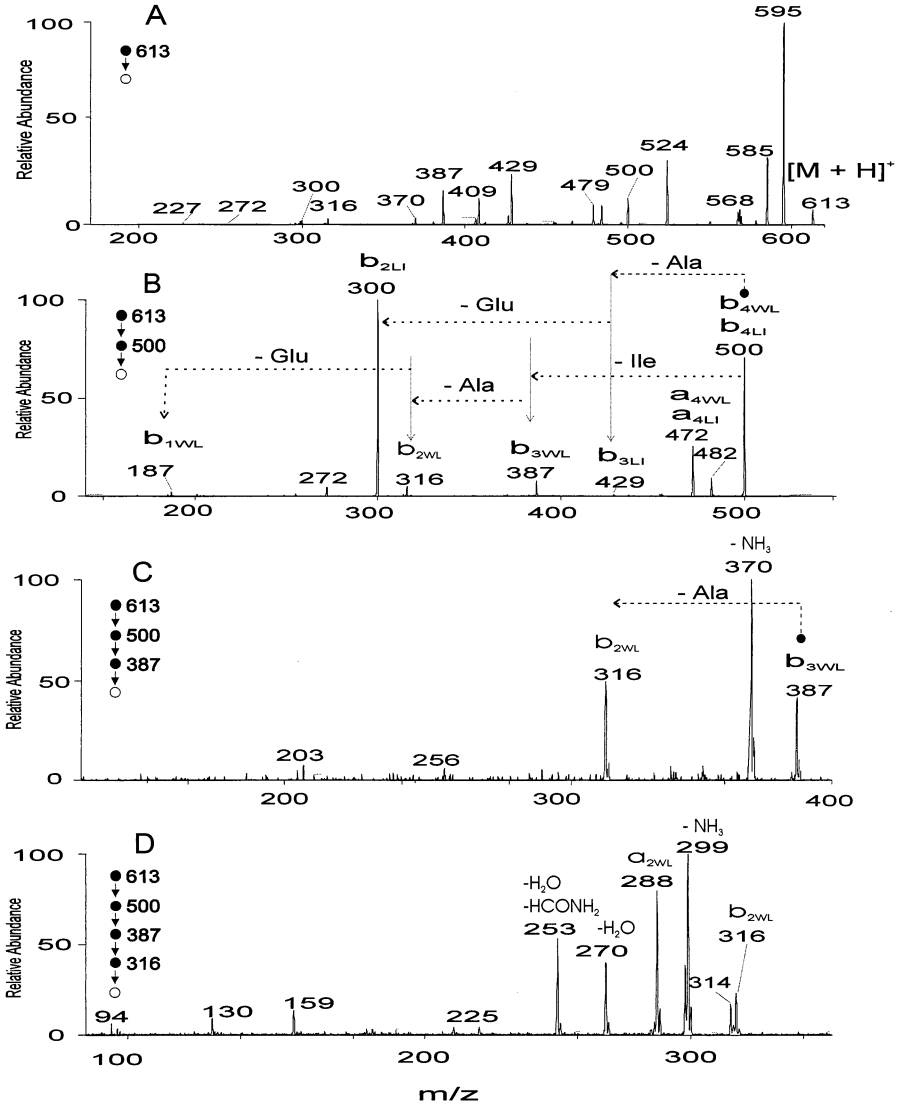

Figure 6. Multistep CAD mass spectra of cyclo(*D*-Glu–Ala–*D*-*allo*Ile–Leu–*D*-Trp). (**A**) First-generation, product-ion spectrum of the protonated molecule. (**B**) Second-generation (MS^3), product-ion spectrum of the b_{4WL} and b_{4LI} ions, HLeu–Trp–Glu–Ala$^+$ and HTrp–Glu–Ala–Ile$^+$, respectively. (**C**) Third-generation (MS^4), product-ion spectrum of the b_{3WL} ion, HTrp–Glu–Ala$^+$. (**D**) Fourth-generation (MS^5), product-ion mass spectrum of the b_{2WL} ion, HTrp–Glu$^+$.

(4%), *m/z* 183 (5%)]; b_{3EW} (*m/z* 314, MS^4) → [*m/z* 299 (16%), *m/z* 296 (70%), *m/z* 286 (30%), *m/z* 268 (25%), *m/z* 243 (40%), b_{2EW}, *m/z* 201 (100%)]; [b_{2EW} *m/z* 201, MS^5] → [*m/z* 183 (100%), a_{2EW}, *m/z* 173 (16%)]; a_{2EW} (*m/z* 173, MS^6) → [*m/z* 155 (100%), *m/z* 101 (45%)]. The facile water losses probably originate at the terminal Glu residue.

Cyclic Peptides Containing Linear Peptide Branches

Collisional activation of a cyclic peptide bearing a linear peptide moiety does not afford cleavage of the cyclic peptide backbone, even when a sodium adduct is

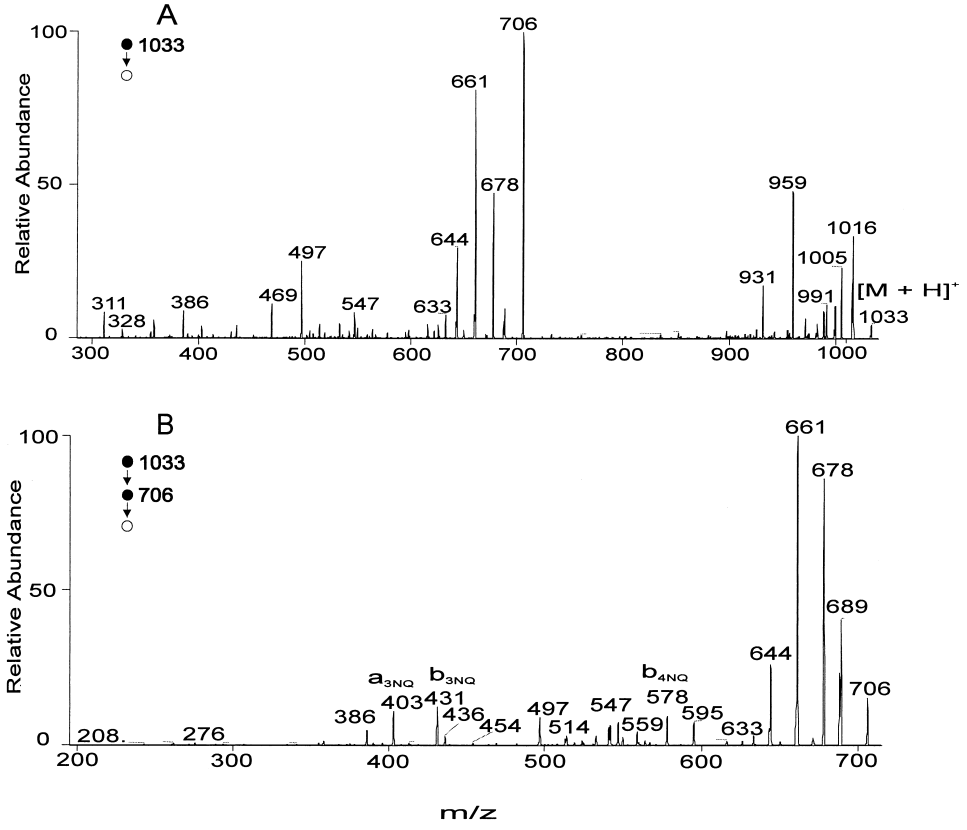

Figure 7. Multistep CAD spectra of cyclo[Tyr–Phe–Gln–Asn–Asu]–Pro–Arg–Gly–NH_2. (**A**) First-generation, product-ion spectrum of the protonated molecule. (**B**) Second-generation (MS^3), product-ion spectrum of the cyclic-peptide moiety at *m/z* 706.

subjected to high-energy, CAD [12]. Thus, a great deal of structural information, including the amino acid sequence of the cyclic peptide moiety, remains inaccessible. The multistage tandem-MS strategy provides a solution to this shortcoming. Applying multiple stages of CAD, we can separate and sequence independently both the linear-peptide and the cyclic-backbone moieties, as was reported earlier [26].

A vasopressin fragment, [$Asu^{1,6}$, Arg^8]-vasopressin, cyclo[Tyr–Phe–Gln–Asn–Asu]–Pro–Arg–Gly–NH_2, is used to illustrate the approach. The peptide consists of eight amino-acid residues, five in the backbone and three in the linear chain. The product-ion spectrum of the $[M + H]^+$ ion (Figure 7) consists of three distinct regions. The molecular-ion region shows that the $[M + H]^+$ at *m/z* 1033 loses small, neutral fragments (NH_3, H_2O, CO, $H_2NCOCH_2NH_2$, and $H_2NCOCH_2NH_2$ and CO). A second region contains information on the cyclic peptide moiety and shows that the small neutral fragments (NH_3, H_2O, CO, $HCONH_2$, $HCONH_2$, and NH_3) are again lost in its fragmentation. The third region of the spectrum contains information on the protonated linear peptide moiety at *m/z* 328. It is desirable that all components of the molecule are present in the spectrum because each can be selected independently and sequenced.

The gas-phase chemistry leading to the formation of the ions is highly dependent on the site of initial protonation to form the $[M + H]^+$. If protonation occurs initially on the proline residue, the linear peptide moiety should be ejected as a neutral species **H**Pro–Arg–Gly–NH_2, and the cyclic peptide moiety, cyclo-(Gln–Asn–Asu^+–Tyr–Phe), is formed as seen in the spectrum by the peak corresponding to the acylium ion or its equivalent at *m/z* 706 (we depict protonation to occur at the nitrogen as a matter of convenience, realizing that the more favored site of protonation is the carbonyl group). On the other hand, when protonation occurs on the linear peptide chain, the linear peptide moiety is produced as seen by the peak for [HPro–Arg–Gly–NH_2 + H]$^+$ at *m/z* 328. In this scenario, the proline residue is protonated by the amide hydrogen of Asu via an intramolecular proton transfer, resulting in the cyclization of the Asu residue to form a bicyclic neutral ketone. The peptide backbone is not observed in the spectrum because it is lost as a neutral species. Both reactions are illustrated in Scheme **2**.

Why don't the relative abundances of the side chain at *m/z* 328 and the backbone at *m/z* 706 correlate with the known basicities of arginine and proline, respectively [32–34]? The answer may be that the displace-

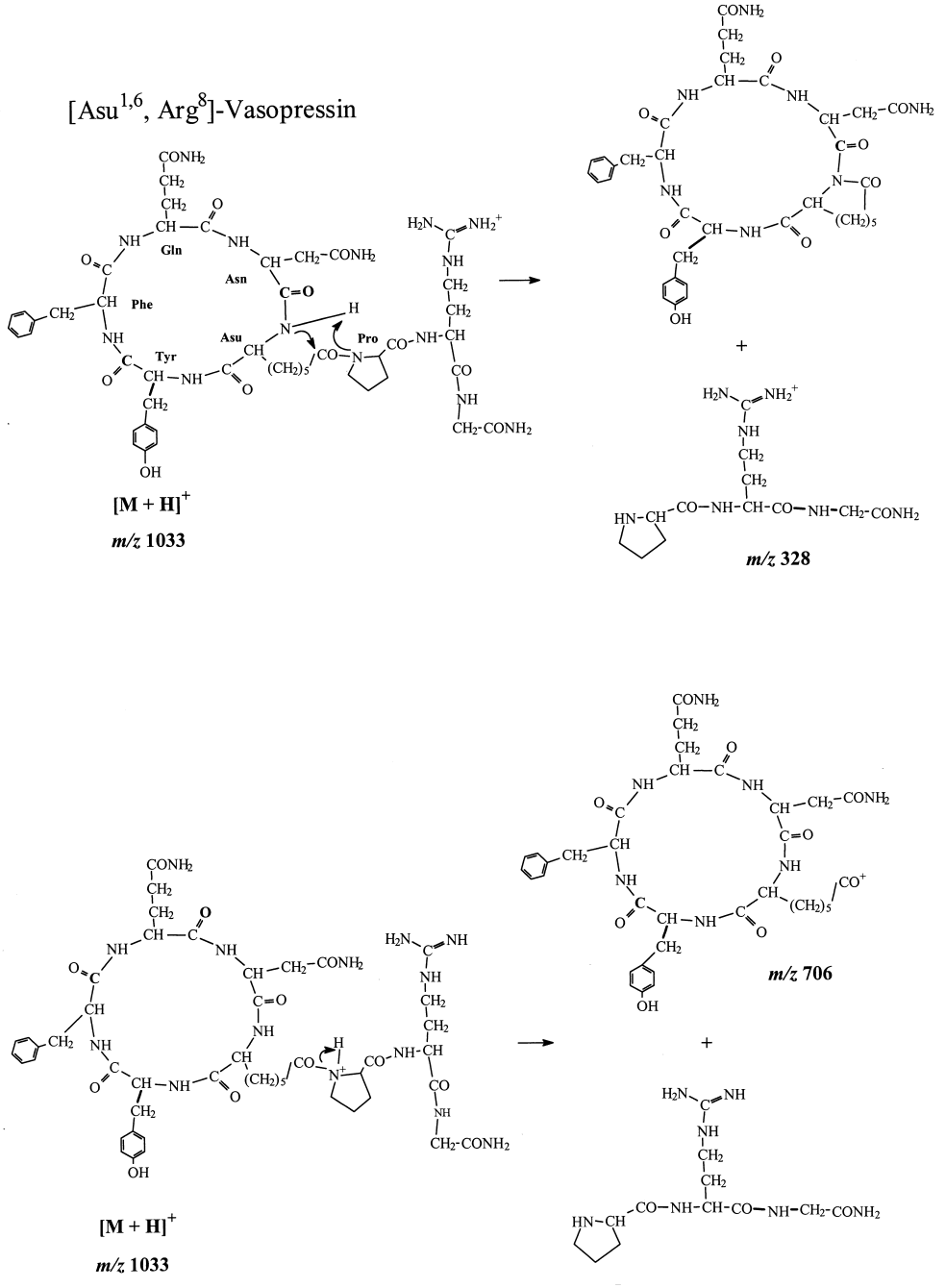

Scheme 2

ment of the linear peptide is limited by the rate of intramolecular protonation of proline nitrogen.

The cyclic peptide moiety at *m/z* 706 was collisionally activated in an MS^3 experiment to produce the second-generation, product-ion spectrum shown in Figure 7B. The product acylium ion (or isomeric equivalent) HAsn–Asu–Tyr–Phe–Gln^+ was then selected and sequenced down to b_{2NQ} (Figure 8A,B,C). In this way, interpreting the complexity of the spectrum in Figure 7B is avoided and establishing the sequence is relatively straightforward by multistep MS/MS. The fragment representing the linear tripeptide moiety, HPro–Arg–Gly–NH_2 + $H]^+$ at *m/z* 328, was selected after one stage of collisional activation and sequenced separately. In an MS^3 experiment, loss of the C-terminal glycine residue to produce the dipeptide b_2 ion HPro–Arg^+ at *m/z* 254 was the dominant reaction path. Further collisional activation in an MS^4 experiment did not produce a b_1 ion (the protonated proline residue). Instead, the b_2 ion loses $(NH_2)_2C{=}NH$ from the arginine side chain.

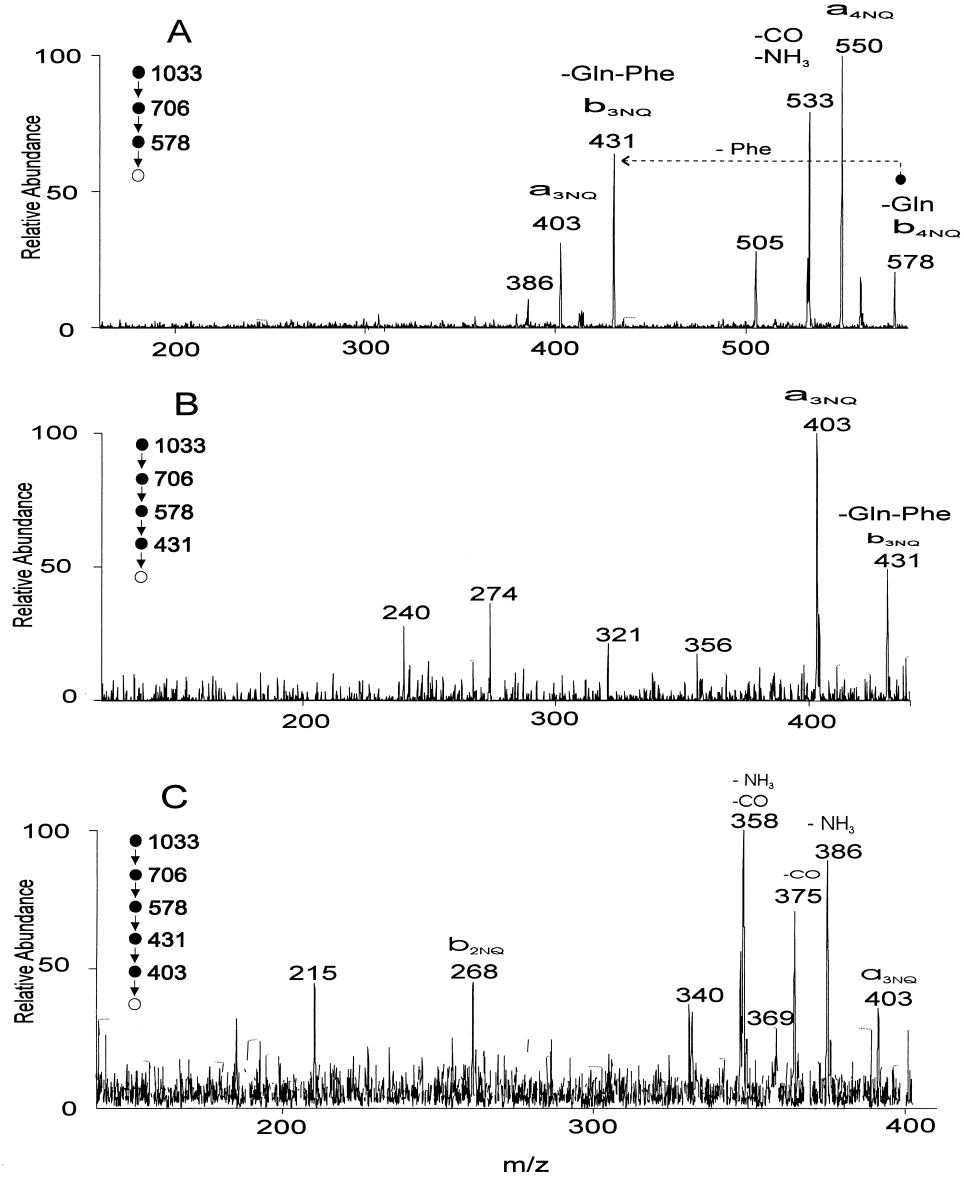

Figure 8. Multistep CAD mass spectra of cyclic-peptide moiety cyclo[Tyr–Phe–Gln–Asn–Asu$^+$]. (**A**) Third-generation (MS^4), product-ion spectrum of the b_{4NQ} ion HAsn–Asu–Tyr–Phe$^+$ formed by ring cleavage at the Asn–Gln amide bond. (**C**) Fourth-generation (MS^5), product-ion mass spectrum of the b_{3NQ} ion, HAsn–Asu–Tyr$^+$. (**D**) Fifth-generation (MS^6), product-ion spectrum of the a_{3NQ} ion formed by decarbonylation of the b_{3NQ}, HAsn–Asu–Tyr$^+$.

Cyclic Peptides Containing Modified Amino Acid Residues

The last example is tentoxin [cyclo(Gly–NMeAla–Leu–dehydro *N*MePhe)], a representative cyclic peptide containing modified amino acid residues (the CAD mass spectra are not shown). Tentoxin presents a unique case for two reasons. First, tentoxin has proven particularly difficult to sequence correctly by mass spectrometry because it has three amino acids: Gly, *N*MeAla, and Leu, that differ by 28 mass units. As a result, there are three sets of isomeric dipeptide moieties and some a ions that have the same nominal mass (Table 1). The

Table 1. Possible isobaric fragment ions (assuming unknown connectivity and orientation) in a CAD mass spectrum of protonated tentoxin

Amino acid residue	b_n(*m/z*)	a_n(*m/z*)
Gly	58	30
NMeAla	86	58
Leu	114	86
Gly–NMeAla or NMeAla–Gly	143	115
NMeLeu–Leu or Leu–NMeAla	199	171
Gly–Leu or Leu–Gly	171	143

difference between the a and b ions can be resolved by exact-mass measurements [35]. The multistep CAD strategy obviates these difficulties, including the requirement for exact-mass measurements, and tentoxin can be sequenced in a straightforward manner.

The second point about tentoxin is that we obtained sequence information for this molecule down to a b_1 ion. In the preceding examples, b_2 ions did not fragment further to furnish b_1 ions upon collisional activation. Tentoxin is an exception; it fragments smoothly to an a_1 ion. [In the nomenclature for labeling fragment ions, the modified amino-acid residues in tentoxin are coded as: dehydro-*N*-Me-phenylalanine (F′); *N*-Me-alanine (A′)]. The product-ion mass spectrum of protonated tentoxin is a summation spectrum, consisting of random fragments arising from ring opening at the Leu–*N*-MeAla, *N*-MeAla–Gly, and (*dehydro*)*N*-MePhe–Leu amide bonds. The ring-opened form of H(*dehydro*)*N*-MePhe–Gly–*N*-MeAla–Leu$^+$ that results from ring scission at the (*dehydro*)*N*-MePhe–Leu amide bond fragments to give the b_{3FL} ion H(*dehydro*)*N*-MePhe–Gly–*N*-MeAla$^+$. The b_{3FL} ion was selected from this spectrum and sequenced down to the a_{1FL} ion at *m/z* 132 in six steps of consecutive CAD: b_{3FL} (*m/z* 415, MS^3) → [a_{3FL} *m/z* 274 (24%), b_{2FL} *m/z* 217 (100%)]; b_{2FL} (*m/z* 217, MS^4) → [a_{2FL} *m/z* 189 (100%)]; a_{2FL} (*m/z* 189, MS^5) → [b_{1FL} *m/z* 160 (20%), *m/z* 146 (100%), a_{1FL} *m/z* 132 (80%), *m/z* 120 (10%), *m/z* 111 (30%)]; b_{1FL} (*m/z* 160, MS^6) → [a_{1FL} *m/z* 132 (100%)].

Competing Side Reactions

The CAD mass spectra of HPro-Val-Leu-Trp$^+$ (Figures 2B and 4B) and HPro-Ile-Leu-Trp$^+$ (Figure 3B) contain fragment ions arising from intramolecular rearrangements. For both product ions, the C-terminal Trp may cyclize to the N-terminal Pro to form rearranged acylium ions: HLeu-Trp-Pro-Val$^+$ and HLeu-Trp-Pro-Ile$^+$. Both rearranged ions produce sequence ions of *m/z* 397 and 300 by losing Val and Pro and Ile and Pro, respectively. Of all the cyclic peptides studied thus far, only these two acylium ions undergo this rearrangement. This may be related to the presence of Trp residues at the C-termini. Furthermore, only these two ions undergo losses of C_3H_8 from the Leu side chain. It is not clear whether these two reactions are related.

Conclusions

Protonated cyclic peptides generated by ESI can be sequenced stepwise in an ion-trap mass spectrometer by taking advantage of the MS^n capabilities. The procedure involves selecting one of the primary acylium ions in the first generation of product ions and subjecting it to several stages of consecutive CAD. Amino-acid residues are sequentially deleted from the C-terminus, principally one at each stage of the CAD experiment, until b_{2JZ} is reached or the precursor-ion signal is too weak for another stage of CAD. In most cases, CAD of b_{2JZ} did not produce b_{1JZ}, requiring that other approaches be used to obtain the sequence of the two N-terminal amino-acid residues. One solution is to sequence at least two primary acylium ions to establish the complete connectivity of the amino acid residues. Another approach is to select another primary ion and sequence it by the multistep method.

This multistep method usually does not suffer from the mass-range limitations of the ion trap because one or two residues are removed at each step. The use of multistep fragmentations also gradually lowers the low-mass limit so that low-*m/z* product ions can ultimately be observed.

The method is fast and efficient, and obviates the need for chemical derivatization or other cumbersome expedients that consume large amounts of scarce samples. The method also eliminates the need to interpret complicated product-ion spectra such as those produced by high-energy CAD, and requires sample amounts in the picomol range, depending on the number of stages, and the size of the peptide.

For an unknown cyclic peptide, one would examine the product-ion spectrum of the protonated molecular ion for losses of common amino-acid residues. The product ions formed by such losses would then be submitted to higher stages of MS/MS, and the criteria for selecting the appropriate product ion repeated for each successive stage. For all cyclic peptides and especially for cyclic peptides containing unusual amino or hydroxy acids, a preliminary analysis of amino-acid (or hydroxy-acid) composition would be helpful.

Acknowledgments

The Washington University Mass Spectrometry Research Resource is supported by the National Centers for Research Resources of the National Institutes of Health (grant no. 2P41RR00954).

References

1. Storm, D. R.; Rosenthal, K. S.; Swanson, P. E. Polymyxin and related antibiotics. *Annu. Rev. Biochem.* **1977,** *46,* 723–763.
2. Kondo, F.; Matsumoto, H.; Yamada, S.; Ishikawa, N.; Ito, E.; Nagata, S.; Ueno, Y.; Suzuki, M.; Harada, K. Detection and identification of metabolites of mycrocystins formed in vivo in mouse and rat livers. *Chem. Res. Toxicol.* **1996,** *9,* 1355–1359.
3. Satoh, T.; Arami, J. M.; Li, S.; Friedman, T. M.; Gao, J.; Edling, A. E.; Townsend, R.; Koch, U.; Chocksi, S.; Germann, M. W.; Korngold, R.; Huang, Z. Bioactive peptide design based on protein surface epitopes. A cyclic heptapeptide mimics CD4 dormain 1 CC′ loop and inhibits biological function. *J. Biol. Chem.* **1997,** *272,* 12175–12180.
4. Duax, W. L.; Griffin, J. F.; Langs, D. A.; Smith, G. D.; Grouchulski, P.; Pletnev, V.; Ivanov, V. Molecular structure and mechanisms of action of cyclic and linear transport antibiotics. *Biopolymers (Peptide Sci.)* **1996,** *40,* 141–155.
5. Ihara, M.; Ishikawa, M.; Fukuroda, T.; Saeki, T.; Funabashi, K.; Fukami, T.; Suda, H.; Yano, M. In vitro biological profile of a highly potent novel endothelin (ET) antagonist BQ-123 selective for the ETA receptor. *J. Cardiovasc. Pharmacol.* **1992,** *20,* S11–S14 (Suppl 1).

6. Yiotakis, A.; Lecoq, A.; Vassiliou, S.; Raynal, I.; Cuniasse, P.; Dive, V. Cyclic peptides with a phosphinic bond a potent inhibitors of a zinc bacterial collagenase. *J. Med. Chem.* **1994,** *37*, 2713–2720.
7. Gross, M. L.; McCrery, D.; Crow, F.; Tomer, K. B.; Pope, M. R.; Cuifetti, L. M.; Knoch, H. W.; Daly, J. M.; Dunkle, L. D. The structure of the toxin from *Helminthosporium carbonum. Tetrahedron. Lett.* **1982,** *23*, 5381–5384.
8. Tomer, K. B.; Crow, F. W.; Gross, M. L. Fast atom bombardment combined with tandem mass spectrometry for the determination of cyclic peptides. *Anal. Chem.* **1984,** *56*, 880–886.
9. Eckart, K.; Schwarz, H.; Tomer, K. B.; Gross, M. L. Tandem mass spectrometry methodology for the sequence determination of cyclic peptides. *J. Am. Chem. Soc.* **1985,** *107*, 6765–6769.
10. Eckart, K. Mass spectrometry of cyclic peptides. *Mass Spectrom. Rev.* **1994,** *13*, 23–55.
11. Ngoka, L. C. M.; Gross, M. L. Location of sodium binding sites in endothelin A selective receptor antagonists cyclo (D-Trp-D-Asp-Pro-D-Val-Leu) and cyclo (D-Trp-D-Asp-Pro-D-Ile-Leu) by multistep collisionally-activated decomposition in an electrospray ion-trap mass spectrometer, in preparation.
12. Ngoka, L. C. M.; Gross, M. L.; Toogood, P. L. Sodium-directed selective cleavage of lactones: A method for structure determination of cyclodepsipeptides. *Int. J. Mass Spectrom. Ion Processes* **1999,** *182/183*, 289–298.
13. Bean, J. W.; Peishoff, C. E.; Kopple, K. D. Conformations of cyclic pentapeptide endothelin receptor antagonists. *Int. J. Peptide Protein Res.* **1994,** *44*, 223–232.
14. Calcagni, A.; Kajtar-Peredy, M.; Lucente, G.; Luisi, G.; Pinnen, F.; Radics, L.; Rossi, D. Nine-membered cyclodepsitripeptides containing the retroisomeric sequence of ergot peptides. *Int. J. Peptide Prot. Res.* **1993,** *42*, 84–92.
15. Coles, M.; Sowemimo, V.; Scanlon, D.; Munro, S. L.; Craik, D. J. A conformation study by 1H NMR of a cyclic pentapeptide antagonist of endothelin. *J. Med. Chem.* **1993,** *36*, 2658–2665.
16. Fesik, S. W.; Bolis, G.; Sham, H. L.; Olejniczak, E. T. Structure refinement of a peptide from two-dimensional NMR data and molecular modeling. *Biochemistry* **1987,** *26*, 1851–1859.
17. Kessler, H.; Klein, M.; Wagner, K. Peptide conformation. 48. Conformation and biological activity of proline containing cyclic retro-analogues of somatostatin. *Int. J. Peptide Prot. Res.* **1988,** *31*, 481–498.
18. Mazzeo, M.; Isernia, C.; Rossi, F.; Saviano, M.; Pedone, C.; Paolillo, L.; Benedetti, E.; Pavone, V. Conformational behavior of a cyclolinopeptide A analogue: Two-dimentional NMR study of cyclo (Pro1-Pro-Phe-Phe-Ac_6c-Ile-Ala-Val_8). *J. Peptide Sci.* **1995,** *1*, 330–340.
19. Saether, O.; Craik, D. J.; Campbell, I. D.; Sletten, K.; Juul, J.; Norman, D. G. Elucidation of the primary and three-dimensional structure of the uterotonic polypeptide kalata B1. *Biochemistry* **1995,** *34*, 4147–4158.
20. Despeyroux, D.; Bordas-Nagy, J.; Jennings, K. R. Determination of amino acid sequence of cystine-containing peptides by tandem mass spectrometry. *Rapid Commun. Mass Spectrom.* **1991,** *5*, 156–159.
21. Reinhold, V. N.; Sheeley, D. M. Detailed characterization of carbohydrate linkage and sequence in an ion trap mass spectrometer: Glycosphingolipids. *Anal. Biochem.* **1998,** *259*, 28–33.
22. Weiskopf, A. S.; Vouros, P.; Harvey, D. J. Characterization of oligosaccharide composition and structure quadrupole ion trap mass spectrometry. *Rapid Commun. Mass Spectrom.* **1997,** *11*, 1493–1504.
23. Nourse, B. D.; Cox, K. A.; Morand, K. L.; Cooks, R. G. Collisional activation of pyrene and anthracene in an ion-trap mass spectrometer. *J. Am. Chem. Soc.* **1992,** *114*, 2010–2016.
24. Strife, R. J.; Ketcha, M. M.; Schwartz, J. Multi-stage mass spectrometry for the isolation and structure elucidation of components of a crude extract. *J. Mass Spectrom.* **1997,** *32*, 1226–1235.
25. Gross, M. L. Tandem mass spectrometry: Multisector magnetic instruments. In *Methods In Enzymology*; McCloskey, J. A., Ed.; Academic: San Diego, 1990; Vol 193, pp 131–153.
26. Ngoka, L. C. M.; Gross, M. L. A nomenclature system for labeling cyclic peptide fragments. *J. Am. Soc. Mass Spectrom.* **1999,** *10*, 360–363.
27. Yalcin, T.; Khouw, C.; Csizmadia, I. G.; Peterson, M. R.; Harrison, A. G. Why are B ions stable species in peptide spectra. *J. Am. Soc. Mass Spectrom.* **1995,** *6*, 1165–1174.
28. Biemann, K. Nomenclature for peptide fragment ions In *Methods in Enzymology*; McCluskey, J. A., Ed.; Academic: Orlando, 1990; Vol 193, pp 886–888.
29. Johnson, R. S.; Martin, S. A.; Biemann, K. Collision-induced fragmentation of $(M + H)^+$ ions of peptides. Side chain specific sequence ions. *Int. J. Mass Spectrom. Ion Processes* **1988,** *86*, 137–154.
30. Johnson, R. S.; Martin, S. A.; Biemann, K.; Stults, J. T.; Watson, J. T. Novel fragmentation process by collision-induced decomposition in a tandem mass spectrometer: Differentiation of leucine and isoleucine. *Anal. Chem.* **1987,** *59*, 2621–2625.
31. Stults, J. S.; Watson, J. T. Identification of a new type of fragment ion in the collisional activation spectra of peptides allows leucine/isoleucine differentiation. *Biomed. Environ. Mass Spectrom.* **1987,** *14*, 583–586.
32. Bojesen, G. The order of proton affinities of the 20 common L-alpha-amino acids. *J. Am. Chem. Soc.* **1987,** *109*, 5557–5558.
33. Cooks, R. G.; Patrick, J. S.; Kotiaho, T.; McLuckey, S. A. Thermochemical determination by the kinetic method. *Mass Spectrom. Rev.* **1994,** *13*, 287–339.
34. Gorman, G. S.; Speir, J. P.; Turner, C. A.; Amster, I. J. Proton affinities of the 20 common alpha-amino acids. *J. Am. Chem. Soc.* **1992,** *114*, 3986–3988.
35. Eckart, K.; Schwarz, H. Sequencing of tentoxin by using fast-atom bombardment (FAB)/high resolution (HR)/tandem mass spectrometry (MSMS). Scope and limitation of a novel strategy. *Helv. Chim. Acta* **1987,** *70*, 489–498.